Rees, D. A. (1963) *Biochem. J. 88*, 343–345.
Robbins, P. W., & Lipmann, F. (1956) *J. Am. Chem. Soc. 78*, 2652–2653.
Schaffer, R., & Isbell, H. S. (1963) *Methods Carbohydr. Chem. 2*, 11–12.
Schircks, von B., Bieri, J. H., & Viscontini, M. (1976) *Helv. Chim. Acta 59*, 248–252.
Terho, T. T., & Harliala, K. (1971) *Anal. Biochem. 41*, 471–476.
Thompson, J. A., Markey, S. P., & Fennessey, P. V. (1975) *Clin. Chem. 21*, 1892–1898.
Tobias, S., Günther, H., & Pfleiderer, W. (1985) *Chem. Ber. 118*, 354–362.
Van Beelen, P., Stassen, A. P. M., Bosch, J. W. G., Vogels, G. D., Guijt, W., & Haasnoot, C. A. G. (1984) *Eur. J. Biochem. 138*, 563–571.
Vogels, G. D., Van Beelen, P., Keltjens, J. T., & Van Der Drift, C. (1984) in *Microbial Growth on C_1 Compounds* (Crawford, R. L., & Hanson, R. S., Eds.) pp 182–187, American Society for Microbiology, Washington, DC.

Interaction of Plant Viruses and Viral Coat Proteins with Mixed Model Membranes†

Klaas P. Datema,*,‡ Ruud B. Spruijt,‡ Benedictus J. M. Verduin,§ and Marcus A. Hemminga‡
Departments of Molecular Physics and Virology, Agricultural University, 6703 BC Wageningen, The Netherlands
Received November 13, 1986; Revised Manuscript Received May 4, 1987

ABSTRACT: The interaction between model membranes and viruses, empty capsids, and coat protein dimers has been investigated. Spherical plant viruses (cowpea chlorotic mottle virus, brome mosaic virus, and southern bean mosaic virus), a rod-shaped plant virus (tobacco mosaic virus), and well-defined aggregation states of their proteins have been used. Turbidity measurements at 550 nm of neutral and positively and negatively charged small unilamellar vesicles interacting with viral material indicated electrostatic and indirect hydrophobic interactions. Electrostatic interaction resulted in lipid–protein complexes, which precipitate. Indirect hydrophobic interaction produced precipitates which contained lipid but no protein. Virus particles and empty capsids of the spherical viruses reacted with charged vesicles through electrostatic interaction. Coat protein dimers of all plant viruses induced vesicle fusion by interaction of the exposed hydrophobic protein domains with neutral vesicles. Further characterization of the precipitates by ^{31}P nuclear magnetic resonance and electron microscopy indicated that both interactions resulted in formation of multilayer structures. Protein assays after incubation at various salt concentrations showed that protein was never incorporated into the bilayer to form a stable complex held together by direct hydrophobic lipid–protein interactions. From the results, it is concluded that such hydrophobic lipid–coat protein interactions do not occur, although hydrophobic protein domains are able to destabilize membranes and induce fusion.

The initial stages of nonenveloped plant virus infection involve penetration of the virus into the cell and subsequent dissociation of the nucleoprotein particle. Conclusions about the site and mechanism of penetration are still controversial. Various components of the cell are reported to affect the dissociation of plant virus particles: the cell wall (Gaard & De Zoeten, 1979; De Zoeten, 1981), the plasma membrane (Kiho et al., 1976, 1979a,b), lipids (Kiho et al., 1980; Banerjee et al., 1981a,b; Abdel-Salam et al., 1982), protoplast membranes (Watts et al., 1981; Watts & King, 1984; Hull & Maule, 1985), and ribosomes (Wilson, 1984).

At present, several models for initial interactions between virus and cell exist. By analogy with the observation that hydrophobic intersubunit bonds play a role in tobacco mosaic virus (TMV)[1] nucleocapsid assembly, it was proposed that a hydrophobic environment is involved in the uncoating of the viral RNA in vivo (Caspar, 1963). Also, divalent cations have been suggested to regulate assembly and disassembly (Durham et al., 1977). Using this observation, a model including both virus penetration and uncoating was postulated, in which the coat protein subunits become integral membrane proteins stabilized by hydrophobic lipid–protein interactions (Durham, 1978). This model is proven for the filamentous bacteriophage M13, in which the coat protein is assumed to span the cytoplasmic bilayer of *Escherichia coli* during a particular stage of infection (Marvin & Wachtel, 1975). Recently, Wilson (1985) suggested a cotranslational disassembly of destabilized TMV and SBMV as a mechanism for uncoating of viral nucleic acid, and evidence was presented that TMV particles disassemble cotranslationally in vivo (Shaw et al., 1986).

We investigated the nature of the interaction (hydrophobic or electrostatic) between artificial membranes and several plant viruses and their coat proteins to mimic and determine the role of the lipid component of the host plasma membrane in initial

† This work was supported by the Netherlands Foundation for Biophysics with financial aid from the Netherlands Organization for the Advancement of Pure Research (ZWO).
* Correspondence should be addressed to this author.
‡ Department of Molecular Physics.
§ Department of Virology.

[1] Abbreviations: TMV, tobacco mosaic virus; CCMV, cowpea chlorotic mottle virus; BMV, brome mosaic virus; SBMV, southern bean mosaic virus; DLPC, dilauroylphosphatidylcholine; DLPA, dilauroylphosphatidic acid; DMPG, dimyristoylphosphatidylglycerol; PALCHOL, palmitoylcholine iodide; CTAB, cetyltrimethylammonium bromide; SUVs, small unilamellar vesicles; SDS–PAGE, sodium dodecyl sulfate–polyacrylamide gel electrophoresis; p*I*, isoelectric point; A_{550nm}, turbidity at 550 nm; EM, electron microscopy; NMR, nuclear magnetic resonance; ppm, parts per million; CSA, chemical shift anisotropy; $\Delta\nu_{1/2}$, line width at half-height; EDTA, ethylenediaminetetraacetic acid; Tris-HCl, tris(hydroxymethyl)aminomethane hydrochloride.

0006-2960/87/0426-6217$01.50/0

interactions. Spherical plant viruses (CCMV, BMV, and SBMV), a rod-shaped plant virus (TMV), and several well-characterized aggregation states of their proteins were used. Binding to negatively charged, neutral, and positively charged small unilamellar vesicles (SUVs) was studied. This binding was measured by the change in turbidity at 550 nm caused by aggregation, fusion, and transformation to multilayer vesicles. Protein content determinations, ^{31}P NMR, and electron microscopy were used for characterization of the aggregation products. The results are discussed with respect to previously proposed models of initial interactions.

Materials and Methods

Chemicals. 1,2-Didodecanoyl-*sn*-glycero-3-phosphocholine (dilauroylphosphatidylcholine, DLPC, 99% purity), 1,2-didodecanoyl-*sn*-glycero-3-phosphatidic acid (dilauroylphosphatidic acid, DLPA, 98% purity), 1,2-ditetradecanoyl-*sn*-glycero-3-phosphoglycerol (dimyristoylphosphatidylglycerol, DMPG, 99% purity), and palmitoylcholine iodide [$C_{16}H_{33}OC_2H_4N^+(CH_3)_3I^-$, PALCHOL] were obtained from Sigma Chemical Co., St. Louis. Cetyltrimethylammonium bromide ($C_{19}H_{42}N^+Br^-$, CTAB, 99% purity) was obtained from Serva Feinbiochemica GMBH & Co., Heidelberg. Lipids and fatty acids were used without further purification.

Sample Preparation. (*A*) *Vesicle Stock Suspensions.* Vesicle stock suspensions of 5.33 mg/mL DLPC (neutral vesicles) and 80/20 w/w mixtures of DLPC/DLPA, DLPC/DMPG (negatively charged vesicles) and of DLPC/PALCHOL, DLPC/CTAB (positively charged vesicles) were prepared in the various buffers also used for solutions of virions and coat protein. DLPC was chosen as bulk lipid since pure DLPC vesicles have the gel to liquid-crystalline phase transition at 0 °C. A clear suspension of SUVs was obtained by sonication under N_2 on ice for 5 min with a Branson B30 cell disruptor [duty cycle, 90%; power setting, 4 (maximum of 350 W at setting 10)]. This resulted in vesicle solutions with $A_{550nm} < 0.1$. After sonication, the pH of the vesicle solution was checked, and no changes were found.

(*B*) *Virus and Coat Protein Stock Solutions.* Viruses were purified as described for TMV (Leberman, 1966), CCMV and BMV (Verduin, 1978), and SBMV (Van Lent & Verduin, 1985). Coat protein was prepared as reported for TMV (De Wit et al., 1978) and for CCMV and BMV (Verduin, 1974). For the preparation of SBMV protein, the virus was first swollen in 10 mM EDTA, pH 8.0, and then treated like CCMV and BMV. Proteins of CCMV, BMV, and SBMV lacking the N-terminal arm were obtained by trypsin treatment and checked with SDS–PAGE as reported earlier (Vriend et al., 1981). A schematic representation of the plant viruses and the various aggregation states of their proteins is shown in Figure 1. The numbers in this figure correspond to the following 4 mg/mL stock solutions: (1) TMV virions in 50 mM sodium acetate/150 mM NaCl, pH 5.0, and in 50 mM potassium phosphate/150 mM NaCl, pH 7.0; (2) TMV protein in 50 mM sodium acetate/150 mM NaCl, pH 5.0, mainly helix form (De Wit et al., 1978, 1979); (3) TMV protein in 50 mM potassium phosphate/150 mM NaCl, pH 7.0, mainly disk form (De Wit et al., 1978, 1979); (4) TMV protein in 50 mM Tris-HCl/150 mM NaCl, pH 9.0, mainly oligomers (De Wit et al., 1978, 1979); (5) CCMV, SBMV, or BMV virions in 50 mM sodium acetate/150 mM NaCl, pH 5.0, and in 50 mM potassium phosphate/150 mM NaCl, pH 7.0; (6) empty capsids of CCMV, SBMV, or BMV protein in 50 mM sodium acetate/200 mM NaCl, pH 5.0; (7) dimers of CCMV, SBMV, or BMV protein in 50 mM Tris-HCl/200 mM NaCl, pH 7.5; (8) empty capsids of CCMV, SBMV, or BMV protein lacking the N-terminal are in 50 mM sodium acetate/200 mM NaCl, pH 5.0; (9) dimers of CCMV, SBMV, or BMV protein lacking the N-terminal arm in 50 mM Tris-HCl/200 mM NaCl, pH 7.5. Coat protein stock solutions were kept at 4 °C and used within 7 days after preparation.

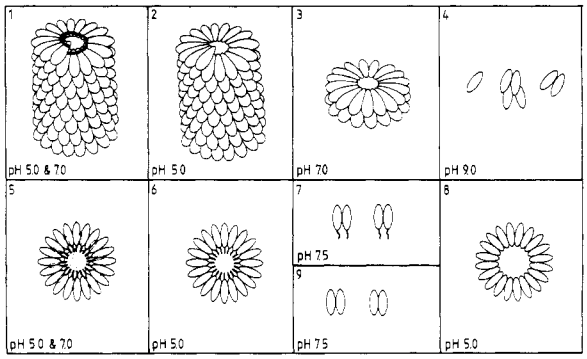

FIGURE 1: Schematic representation of the plant viruses and various aggregation states of their coat proteins. Rod-shaped TMV virions (1); TMV protein in helix form (2), in disk form (3), and as oligomers (4). Spherical CCMV, SBMV, or BMV virions (5), empty capsids of CCMV, SBMV, or BMV protein (6), dimers of CCMV, SBMV, or BMV protein (7), empty capsids of CCMV, SBMV, or BMV protein lacking the N-terminal arm (8), and dimers of CCMV, SBMV, or BMV protein lacking the N-terminal arm (9). Numbers correspond to the numbering used for stock solutions of virus and coat proteins (see Materials and Methods).

(*C*) *Samples for Turbidity Measurements at 550 nm and Electron Microscopy.* The samples for turbidity measurements at 550 nm were prepared by adding 250 μL of virus or protein stock solution to 750 μL of vesicle stock suspension in the same buffer. The final concentration of lipid was 4 mg/mL of buffer and of the virus or coat protein 1 mg/mL of buffer. During a 24-h period, the 1-mL samples were incubated at 18 °C. The samples were measured at 1-h intervals. For each turbidity measurement, the samples were transferred to a quartz cuvette. After incubation for turbidity measurements at 550 nm, aliquots of the mixed samples were taken for electron microscopy.

(*D*) *Samples for ^{31}P NMR.* A unilamellar DLPC vesicle solution (5.33 mg of lipid/mL) was prepared in 10 mM Tris-HCl/150 mM NaCl/1 mM EDTA, pH 9.0, by sonication in two 15-mL portions as described under section A. Titanium particles of the sonicator and residual multilamellar vesicles were removed by centrifugation (10000*g*, 15 min). The supernatants were mixed, resulting in a single homogeneous clear unilamellar DLPC vesicle suspension of 30 mL. One 15-mL fraction was incubated with 5 mL of TMV protein stock sol ution number 4 for 24 h at 18 °C, and the other 15-mL fraction was incubated with 5 mL of identical buffer as reference. Before measurement, samples were concentrated by ultracentrifugation (250000*g*, 1 h), resuspended in 10% (v/v) ^2H_2O containing 10 mM Tris-HCl/150 mM NaCl/1mM EDTA buffer, pH 9.0 (final volume 2 mL), and treated as indicated in Figure 5.

Absorption Measurements. The turbidity of the samples was measured in a Kontron Uvikon 810 spectrophotometer at 550 nm to avoid contributions of absorption of viral material or lipids. Turbidities at 550 nm of identical control vesicle suspensions not exposed to viral material (in all cases less than 0.10) and of viral material were subtracted if necessary.

Determination of the Amount of Protein Associated with Membranes after Incubation. After the 24-h period of incubation of the vesicle suspensions with protein, the aggregated, fused, and multilamellar bilayers together with associated protein were pelleted by centrifugation (8800*g*, 10 min). The fraction of residual, unassociated protein in the supernatant

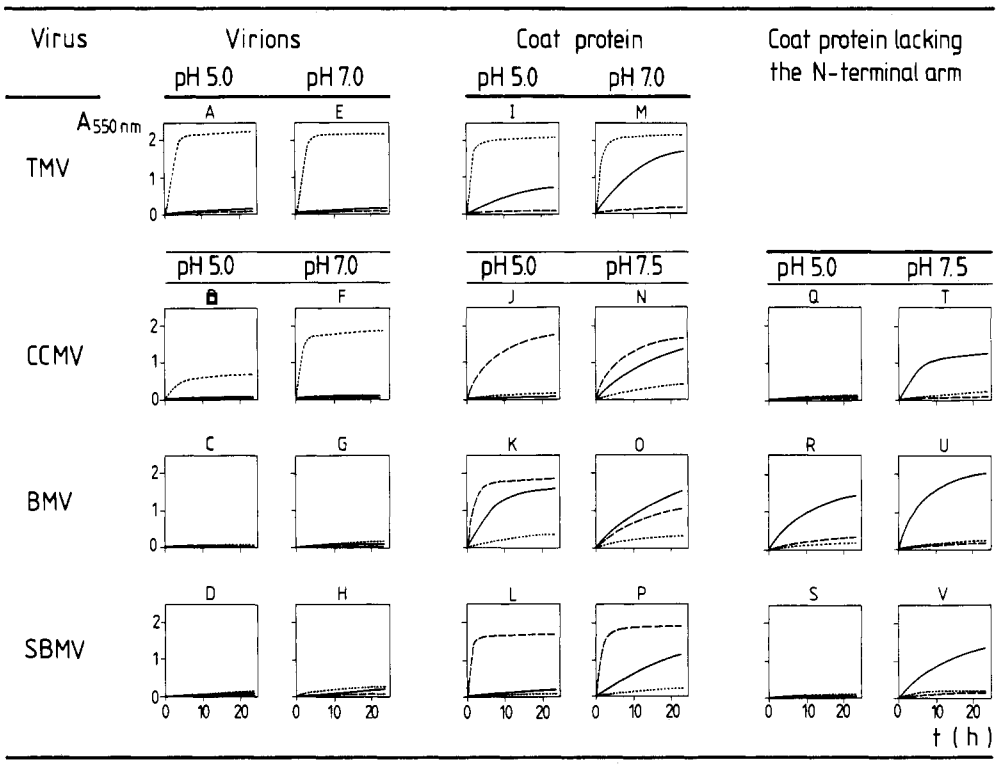

FIGURE 2: Turbidity of suspensions (final lipid concentration 4 mg/mL) of neutral vesicles [100% DLPC (solid line)], positively charged vesicles [80/20 w/w DLPC/CTAB or DLPC/PALCHOL (dotted line)], and negatively charged vesicles [80/20 w/w DLPC/DLPA or DLPC/DMPG (dashed line)] after addition of virions (A–H), protein (I–P), and protein lacking the N-terminal arm (Q–V) of TMV (first row—A, E, I, and M), CCMV (second row—B, F, J, N, Q, and T), BMV (third row—C, G, K, O, R, and U), and SBMV (fourth row—D, H, L, P, S, and V) as illustrated in Figure 1. All experiments were carried out at 18 °C, and the same buffer as for vesicle stock suspensions was used for viral particle or protein stock solutions. (A, I) pH 5.0 in 50 mM sodium acetate/150 mM NaCl buffer; (B–D, J–L, Q–S) pH 5.0 in 50 mM sodium acetate/200 mM NaCl buffer; (E–H, M) pH 7.0 in 50 mM potassium phosphate/150 mM NaCl buffer; (N–P, T–V) pH 7.5 in 50 mM Tris-HCl/200 mM NaCl buffer.

was calculated from the protein contribution at 280 nm in the UV spectrum using an extinction coefficient at 280 nm = 1.27 $mL \cdot mg^{-1} \cdot cm^{-1}$ for TMV, CCMV, and BMV protein and 1.30 $mL \cdot mg^{-1} \cdot cm^{-1}$ for SBMV protein. This fraction was subtracted from the 1 mg of protein initially added to obtain the complementary fraction of membrane-associated protein presented in Table I.

Electron Microscopy. Electron micrographs were taken with a Zeiss EM 109 electron microscope equipped with a transfiber photography camera. The samples were negatively stained with a 2% solution of uranyl acetate in double-distilled water.

Phosphorus Magnetic Resonance Spectroscopy. The ^{31}P NMR spectra of the DLPC vesicle suspension after 24-h incubation with TMV protein were obtained with a Bruker CXP 300 Fourier transform spectrometer operating at a frequency of 121.48 MHz. The spectra were taken in the presence of broad-band proton decoupling (20 W/12 dB) using a sweep width of 25 000 Hz and a 16-μs 45° pulse with a repetition rate of 1 s.

RESULTS

Turbidity Measurements and Determination of Protein Associated with Membranes. The effect of addition of plant viruses and their coat proteins to neutral and charged SUVs under various conditions was monitored by turbidity measurements at 550 nm. In addition, the percentage of protein present in the pellet was determined after centrifugation of the samples.

(A) Effect of Intact Virions. Addition of TMV or CCMV to positively charged SUVs at pH 5 and 7 increased the turbidity, but not in the case of neutral or negatively charged SUVs (Figure 2A,B,E,F). The turbidity increase for CCMV–lipid mixtures was stronger at pH 7 than at pH 5. In all cases, addition of BMV or SBMV had only a small effect on the turbidity (Figure 2C,D,G,H). Pellets of positively charged SUVs obtained after incubation with TMV at pH 5 and 7 contained all the protein initially added. Pellets of positively charged SUVs obtained after incubation with SBMV at pH 7 and with CCMV at pH 5 and 7 contained approximately 20%, 20%, and 60% of the protein, respectively. In all other pellets, no protein was detected within experimental error (Table I).

(B) Effect of the Proteins. Addition of TMV protein at pH 5, 7 (Figure 2I,M), and 9 (data not shown) to positively charged SUVs increased the turbidity rapidly. No increase of turbidity was found with negatively charged SUVs. Neutral SUVs caused a much slower increase of the turbidity as compared to the positively charged SUVs. The turbidity 24 h after incubation increased as a function of pH from 5 to 9. Only in pellets of positively charged SUVs obtained after incubation with TMV protein, all the initially added coat protein was found (Table I).

Addition of CCMV, BMV, and SBMV protein at pH 5 and 7.5 to positively charged SUVs had no significant effect on the turbidity (Figure 2J–L and N–P). For negatively charged SUVs, the addition of these proteins increased the turbidity (Figure 2J–L and N–P), and also protein was found in the pellets: 55% ± 10% for CCMV at pH 5.0 and 7.5, 85% ± 10% for BMV and SBMV at pH 5, 20% ± 10% for BMV at pH 7.5, and 55% ± 10% for SBMV at pH 7.5 (Table I). The addition of CCMV, BMV, and SBMV protein increased the turbidity of neutral SUVs at pH 7.5 (Figure 2N–P) and also at pH 5 for BMV protein (Figure 2K). However, no protein

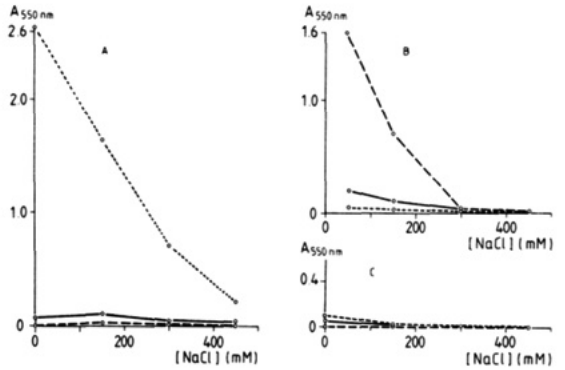

FIGURE 3: Turbidity of suspensions (final lipid concentration 4 mg/mL) of neutral vesicles [100% DLPC (solid line)], positively charged vesicles [80/20 w/w DLPC/PALCHOL (dotted line)], and negatively charged vesicles [80/20 w/w DLPC/DLPA (dashed line)] 30 min after addition of (A) TMV protein in 50 mM potassium phosphate, pH 9.0, (B) CCMV protein in 50 mM Tris-HCl, pH 7.5, and (C) CCMV protein lacking the N-terminal arm in 50 mM Tris-HCl, pH 7.5, as a function of NaCl concentration.

was found in pellets of neutral SUVs (Table I).

(C) Effect of Proteins Lacking the N-Terminal Arm. After removal of the N-terminal arm of the CCMV, BMV, and SBMV protein, no significant changes in turbidity were observed with positively and negatively charged SUVs at pH 5 and 7.5 (Figure 2Q–V). The turbidity changes found for neutral SUVs after incubation with intact CCMV, BMV, and SBMV protein were preserved with the cleaved proteins. Also, cleaved protein was not bound (Table I).

Salt Concentration Dependence of Turbidity Induced by Proteins. The turbidity of the SUV suspensions was measured as a function of NaCl concentration 30 min after addition of TMV protein (Figure 3A), of CCMV protein (Figure 3B), and of CCMV protein lacking the N-terminal arm (Figure 3C). The turbidity was reduced with increasing salt concentration. This effect was most clear for positively charged SUVs incubated with TMV protein (Figure 3A) and for negatively charged SUVs incubated with CCMV protein (Figure 3B).

Table I: Percentage of Coat Protein Associated with Membranes[a]

virus	membrane charge	virions pH 5	virions pH 7	coat protein pH 5	coat protein pH 7	coat protein pH 9
TMV	positive	****	****	****	****	****
	neutral	–	–	–	–	–
	negative	–	–	–	–	–

virus	membrane charge	virions pH 5	virions pH 7	coat protein pH 5	coat protein pH 7.5	coat protein lacking N-terminal arm pH 5	coat protein lacking N-terminal arm pH 7.5
CCMV	positive	*	***	–	–	–	–
	neutral	–	–	–	–	–	–
	negative	–	–	***	***	–	–
BMV	positive	–	–	–	–	–	–
	neutral	–	–	–	–	–	–
	negative	–	–	****	*	–	–
SBMV	positive	–	*	–	–	–	–
	neutral	–	–	–	–	–	–
	negative	–	–	****	***	–	–

[a] Pellets were obtained by centrifugation (8800*g*, 10 min) of the samples of Figure 2 after 24 h of incubation: – = 0–12%, * = 12–25%, ** = 25–50%, *** = 50–75%, and **** = 75–100%. In case of CCMV and SBMV protein, only the values of DLPA SUVs are presented.

Electron Microscopy. After turbidity measurements, electron micrographs were taken of the samples. In Figure 4A, a typical electron micrograph of a reference sample of negatively charged SUVs after 24 h of incubation is shown. The diameter of the SUVs ranges from 30 to 100 nm. Identical vesicle sizes were observed for other reference vesicles (data not shown). After 24 h of incubation of negatively charged SUVs with empty capsids of BMV protein at pH 5 (Figure 4B), multilamellar aggregates were formed.

Typical multilayer structures as in Figure 4B were observed in all electron micrographs (data not shown) taken of samples of which the turbidity at 550 nm had increased to values higher than 1 at the end of the 24-h incubation period after addition of TMV protein or CCMV, BMV, or SBMV protein with or

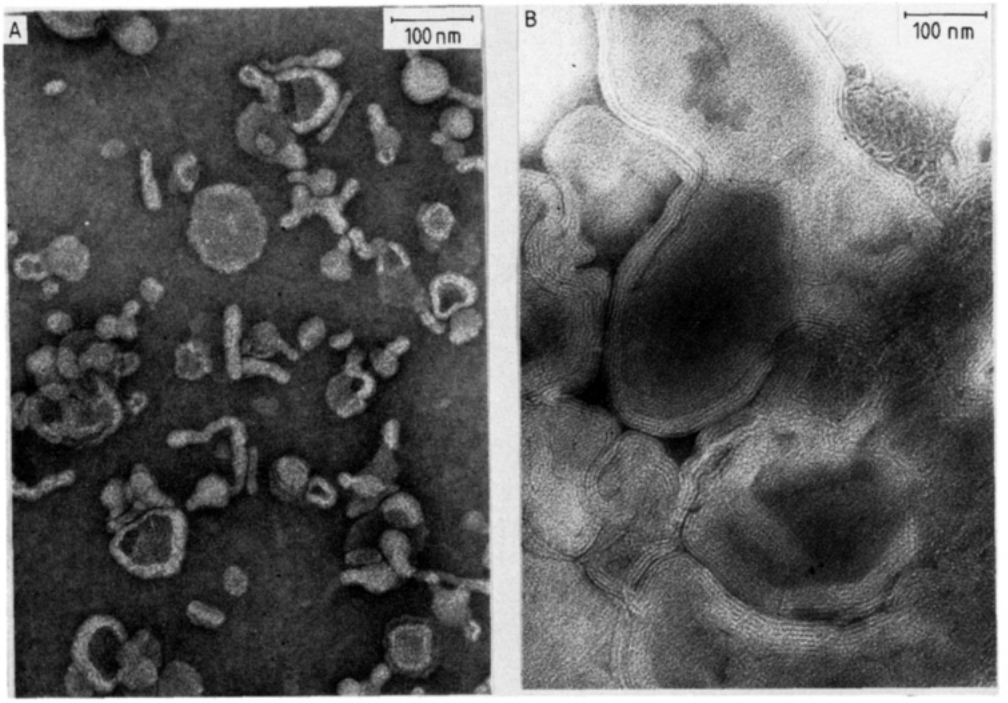

FIGURE 4: Electron micrographs showing the typical shape of unilamellar vesicles after 24 h of incubation of the DLPC/DLPA (80/20 w/w) vesicles (A) and of multilayer structures in the pellet after 24 h of incubation of the DLPC/DLPA (80/20 w/w) vesicles with empty capsids of BMV protein in 50 mM sodium acetate/200 mM NaCl buffer, pH 5.0 (B).

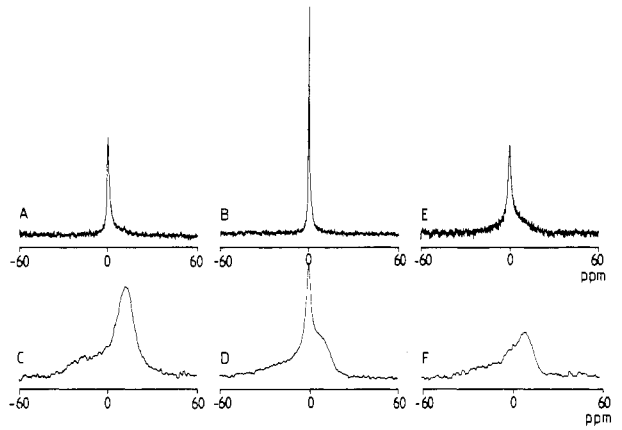

FIGURE 5: 121.48-MHz ^{31}P NMR spectra of a suspension of DLPC SUVs in 10 mM Tris-HCl/150 mM NaCl/1 mM EDTA buffer, pH 9.0, after 24 h of incubation at 18 °C without viral material (A) and (B) sample of (A) after 1 min of sonication; (C) as (A) with TMV protein and (D) sample of (C) after 1 min of sonication; (E) supernatant (8800*g*, 10 min) and (F) pellet (8800*g*, 10 min) of sample (D). In all cases, the number of scans was 1000, and broad-band proton decoupling (20 W/12 dB) was applied. For spectra in (A), (B), and (E), an artificial line broadening of 10 Hz was used, and in (C), (D), and (F), 100 Hz was used.

without an N-terminal arm (Figure 2I–V).

Phosphorus NMR Measurements. Figure 5 shows ^{31}P NMR spectra obtained of DLPC SUVs after 24 h of incubation at 18 °C with and without TMV protein. The spectrum of the reference SUVs is characterized by one isotropic peak with a line width at half-height, $\Delta\nu_{1/2}$, of 190 Hz (Figure 5A). After 1 min of sonication, $\Delta\nu_{1/2}$ decreased to 70 Hz (Figure 5B). An identical sample incubated for 24 h with TMV coat protein gave a typical powder spectrum characteristic for bilayers with a CSA of ca. 30 ppm (Figure 5C). No peaks were visible that could arise from the presence of rapidly tumbling phospholipid molecules (Burnell et al., 1980) or H_{II} phase lipids (Van Echteld et al., 1982). After 1-min sonication of this sample, an isotropic peak with a relative intensity of approximately 20% was seen (Figure 5D). This peak could be separated from the underlying powder spectrum by centrifugation (8800*g*, 10 min). This resulted in an isotropic peak with a $\Delta\nu_{1/2}$ of 370 Hz of the supernatant (Figure 5E) and a powder spectrum of the pellet (Figure 5F) with a CSA of ca. 30 ppm, similar to Figure 5C.

Discussion

The turbidity measurements of neutral and charged SUVs interacting with intact plant viruses or their coat proteins indicated the following.

(*A*) *Electrostatic Interaction.* The virus particle or protein contains charged amino acid residues which interact with oppositely charged membranes. As a consequence, several vesicles are cross-linked. Also, charges at the membrane are neutralized, causing aggregation, vesicle fusion, and formation of multilayer structures. The precipitated material contains viral coat protein.

(*B*) *Indirect Hydrophobic Interaction.* Dissociated protein causes neutral vesicles to fuse and to form multilayer structures. The precipitated material does not contain protein. As will be discussed later, this effect is caused by exposed hydrophobic protein domains.

For the interactions, the following evidence was presented:

(*1*) *Rod-Shaped TMV.* Positively charged vesicles interact with TMV particles at pH 5 and 7 (Figure 2A,E). The same is observed for its coat protein, both in helix and in disk conformation (Figure 2I,M) and as oligomers at pH 9 (data not shown). The pellet contains all coat protein (Table I) whereas multilamellar vesicles are formed (Figure 4B). Several arguments suggest that electrostatic forces dominate in the formation of these pellets: (a) The p*I* of TMV particles is 3.5 (Fraenkel-Conrat & Nariba, 1958). This implies that the virus surface has an overall negative charge at the experimental pH values. (b) Negatively charged SUVs do not interact with TMV and its protein. (c) A reduction of protein–vesicle interaction by high salt concentration is observed by the turbidity measurements at 550 nm as function of salt concentration (Figure 3A).

TMV protein with its hydrophobic areas exposed to the bulk solvent (Bloomer et al., 1978) causes the neutral SUVs to fuse after aggregation (Figure 2I,M). This result agrees with those of Banerjee et al. (1981a,b). In this case, no protein is detectable in the pellet (Table I). This effect parallels the increasing exposure of hydrophobic domains of TMV protein at higher pH values.

An increase in turbidity at 550 nm can only be interpreted as an increase in size of the aggregates. Thus, on the basis of turbidity measurements, no discrimination between aggregation, fusion, or transformation to multilayer structures can be made. Also, spontaneous aggregation of DLPC SUVs after preparation by sonication was reported (De Kruijff et al., 1976), which was observed as a broadening of the ^{31}P NMR signal. Therefore, ^{31}P NMR spectra were recorded, and EM micrographs were taken. After 24 h of incubation of the reference DLPC SUVs, the increased line width (190 Hz) of the ^{31}P NMR resonance indicates aggregation of the SUVs (Figure 5A,B). The electron micrograph of the reference vesicles after 24 h of incubation shows that no transformation to multilayer structures has occurred (Figure 4A). However, after 24 h of incubation with TMV protein, the ^{31}P NMR spectrum indicates that the majority of the vesicles (minimally ca. 80%) has become multilamellar (Figure 5F). The rest (maximally ca. 20%) is aggregated since it appears as a relatively sharp isotropic peak after brief sonication (Figure 5D). These results are in accordance with the multilayer structures observed in electron micrographs of the same samples (data not shown). Formation of multilamellar vesicles implies that fusion of vesicles has taken place.

(*2*) *Spherical Plant Viruses (CCMV, BMV, and SBMV).* In analogy to TMV, CCMV particles interact with positively charged vesicles (Figure 2B,F), which is explained by the p*I* value of 3.6 (Bancroft et al., 1971). As a result of the electrostatic interaction, the pellets of these samples contain protein at pH 5 (ca. 20%) and 7 (ca. 60%, Table I), values at which an increasing number of negatively charged groups per viral particle is present. CCMV protein has an N-terminal arm of 25 amino acid residues of which 9 residues are basic. In dimers as well as in empty capsids this arm is known to bind to negatively charged macromolecules in solution (Bancroft, 1971; Vriend et al., 1986). Therefore, binding to negatively charged vesicles is not surprising (Figure 2J,N). Binding is lost after removal of the N-terminal arm by trypsin (Figure 2Q,T).

Dissociated CCMV protein, with and without the N-terminal arm, induces fusion of neutral SUVs and formation of multilayers (Figure 2N,T). This is analogous to the effect of TMV protein on neutral vesicles (Figure 2I,M).

BMV and SBMV have p*I* values of 6.8 (Magdolf-Fairchild, 1967) and 6.0 (Rice & Horst, 1972), respectively. These viruses do not interact with SUVs, regardless of their surface charge. SBMV is an exception, giving a small electrostatic effect at pH 7, if added to positively charged SUVs (Figure

2C,D,G,H). This binding, which was also demonstrated by Abdel-Salam et al. (1982) in 0.1 M Tris-HCl, pH 7.5, could be due to the swollen state of SBMV. The near-neutral p*I* values of BMV and SBMV are also reflected in the absence of protein association to positive SUVs (Table I). BMV and SBMV protein, either as capsids or as dimers, interact with negatively charged SUVs (Figure 2K,L,O,P) because of the presence of their basic N-terminal arms. This interaction is lost after removal of the arm (Figure 2R,S,U,V).

Both BMV and SBMV protein dimers induce fusion of neutral SUVs (Figure 2O,P), and this inductive capacity is completely preserved after cleavage of the N-terminal arms (Figure 2U,V). Also, BMV empty capsids with and without the N-terminal arm react with neutral SUVs by indirect hydrophobic interaction (Figure 2K,R). This can be attributed to the strong hydrophobic character of BMV protein (Pfeiffer & Hirth, 1974). Again, the induction of vesicle fusion increases with increasing hydrophobicity of the protein.

Nature of the Interaction between Model Membranes and Several Plant Viruses and Their Coat Proteins. In the discussion of the results, electrostatic interaction was found to be quite different from induction of vesicle fusion by indirect hydrophobic interaction.

The electrostatic interactions are reduced to zero at high salt concentration (Figure 3). Therefore, there is no indication of hydrophobic interaction in the formed complex, i.e., between hydrophobic protein domains and the bilayer interior. Thus, the protein is likely to be associated to the head groups of the bilayers. This process is analogous to that found for aggregation and fusion of negatively charged SUVs by polycations, such as polylysine (Gad et al., 1982, 1985) and polyhistidine (Wang & Huang, 1984; Uster & Deamer, 1985).

Induction of vesicle fusion and formation of multilayers by indirect hydrophobic interaction are observed only for neutral vesicles. Neutral SUVs aggregate spontaneously (De Kruijff et al., 1976). This is observed in the ^{31}P NMR spectrum (Figure 5A) as a broadening of the isotropic resonance. Brief sonication reverses this aggregation (Figure 5B). Vesicle fusion and further formation of multilamellar structures are inhibited by interfacial water between the apposed bilayer surfaces of two aggregated vesicles (Le Neveu et al., 1976; Papahadjopoulos et al., 1978). A possible mechanism for the indirect hydrophobic interaction is that the hydrophobic sites at the proteins in the solution remove this hydration water, enabling direct molecular contacts of the bilayers and concomitant fusion according to the general theory of vesicle fusion (Wilschut & Hoekstra, 1986). The proposed effect of the protein can be visualized as a pushing out of the interfacial water, resulting in a partial dehydration of the bilayer surface. This process is slow, since it requires a collision of the protein with already apposed bilayer surfaces. The protein itself is not inserted in the bilayer nor does it form a complex with the lipids. Also, the protein does not pass through the membrane during the fusion process, since otherwise it would have been locked in the fused vesicles and appeared in the final multilayer precipitate. The action of the protein may be compared to that of a catalyst in a chemical reaction, enhancing only the rate of fusion between the bilayers.

Since the coat protein is not found associated with the vesicles in the case of hydrophobic interaction (Table I), this implies that the hydrophobic protein domains do not interact directly with the hydrophobic interior of the bilayers.

From these observations, it is concluded that, regardless of the type of interaction (hydrophobic, electrostatic), viral coat protein is not incorporated in the bilayer, i.e., by forming a stable complex held together by direct hydrophobic lipid–protein interactions.

Implications of the Observed Interactions for Earlier Proposed Models of Initial Interactions between Virus and Cell. A stable lipid–coat protein complex in which direct hydrophobic forces dominate was not found for any of the viruses and bilayers that were investigated. This strongly disagrees with the model of virus penetration and uncoating proposed by Durham (1978), which we therefore consider incorrect.

Caspar (1963) suggested that the hydrophobic environment of the bilayer interior causes uncoating of TMV RNA in vivo. Although this mechanism of uncoating cannot be excluded rigorously, it is very unlikely on the basis of our results. From Figure 2A–H, it is clear that viral particles can interact with the head groups of lipids in the bilayer only by electrostatic interaction, which results in coat protein associated *to the outside* of the bilayer. In the final complex also, no direct hydrophobic forces are involved (Figure 3). Therefore, the uncoating process is definitely not initiated and probably also not propagated by hydrophobic lipid–coat protein forces, replacing the hydrophobic intersubunit forces in the virus particle.

Contrary to the suggested uncoating effect of the hydrophobic domain of the bilayer on the virus (Caspar, 1963), for which no information is available from our experiments that focused on the effect of virus–membrane interactions on the membranes, a destabilizing effect of the hydrophobic domains of the viral coat proteins on the membrane has been observed. This suggests that in vivo the virus particle could induce membrane fusion by exposing its hydrophobic protein domains. This could possibly be a mechanism for the virus to enter the cell.

ACKNOWLEDGMENTS

We thank B. de Kruijff, J. W. Roenhorst, T. J. Schaafsma, and J. Wilschut for valuable discussions and critical reading of the manuscript, C. J. A. M. Wolfs and H. R. Bloksma for help with the preparation of plant virus material, and J. Groenewegen for help with electron microscopy.

REFERENCES

Abdel-Salam, A., White, J. A., & Sehgal, O. P. (1982) *Phytopathol. Z. 105*, 336–334.

Bancroft, J. B. (1971) *Adv. Virus Res. 16*, 99–134.

Banerjee, S., Vandenbranden, M., & Ruysschaert, J. M. (1981a) *Biochim. Biophys. Acta 646*, 360–364.

Banerjee, S., Vandenbranden, M., & Ruysschaert, J. M. (1981b) *FEBS Lett. 133*, 221–224.

Bloomer, A. C., Champness, J. N., Bricogne, G., Staden, R., & Klug, A. (1978) *Nature (London) 276*, 362–368.

Burnell, E. E., Cullis, P. R., & De Kruijff, B. (1980) *Biochim. Biophys. Acta 603*, 63–69.

Caspar, D. L. D. (1963) *Adv. Protein Chem. 18*, 87–121.

De Kruijff, B., Cullis, P. R., & Radda, G. K. (1976) *Biochim. Biophys. Acta 436*, 729–740.

De Wit, J. L., Hemminga, M. A., & Schaafsma, T. J. (1978) *J. Magn. Reson. 31*, 97–107.

De Wit, J. L., Alma, N. C. M., Hemminga, M. A., & Schaafsma, T. J. (1979) *Biochemistry 18*, 3973–3976.

De Zoeten, G. A. (1981) in *Plant Diseases and Vectors* (Maramorosch, K., & Harris, K. F., Eds.) pp 221–239, Academic Press, New York.

Durham, A. C. H. (1978) *Biomedicine 28*, 307–314.

Durham, A. C. H., Hendry, D. A., & Von Wechmar, M. B. (1977) *Virology 77*, 524–533.

Fraenkel-Conrat, H., & Nariba, X. (1958) in *Symposium on Protein Structure* (Neuberger, A., Ed.) p 249, Methuen, London.
Gaard, G., & De Zoeten, G. A. (1979) *Virology 96*, 21–31.
Gad, A. E., Sliver, B. L., & Eytan, G. D. (1982) *Biochim. Biophys. Acta 690*, 124–132.
Gad, A. E., Bental, M., Elyashir, G., & Weinberg, H. (1985) *Biochemistry 24*, 6277–6282.
Hull, R., & Maule, A. J. (1985) in *The Viruses* (Francki, R. I. B., Ed.) pp 83–115, Plenum Press, New York.
Kiho, Y., & Shimomura, T. (1976) *Jpn. J. Microbiol. 20*, 537–541.
Kiho, Y., & Abe, T. (1980) *Microbiol. Immunol. 24*, 617–628.
Kiho, Y., Shimomura, T., Abe, T., & Nozu, Y. (1979a) *Microbiol. Immunol. 23*, 735–748.
Kiho, Y., Abe, T., & Ohashi, Y. (1979b) *Microbiol. Immunol. 23*, 1067–1076.
Leberman, R. (1966) *Virology 30*, 341–347.
Le Neveu, D. M., Rand, R. P., & Parsegian, V. A. (1976) *Nature (London) 259*, 601–603.
Magdolf-Fairchild, B. S. (1967) *Virology 31*, 142–143.
Marvin, D. A., & Wachtel, E. J. (1975) *Nature (London) 253*, 19–23.
Papahadjopoulos, D., Portis, A., Jr., & Pangborn, W. (1978) *Ann. N.Y. Acad. Sci. 308*, 50.
Pfeiffer, P., & Hirth, L. (1974) *Virology 58*, 362–368.
Rice, R. H., & Horst, J. (1972) *Virology 49*, 602–604.
Shaw, J. G., Plaskitt, K. A., & Wilson, T. M. A. (1986) *Virology 148*, 326–336.
Uster, P. S., & Deamer, D. W. (1985) *Biochemistry 24*, 1–8.
Van Echteld, C. J. A., De Kruijff, B., Verkley, A. J., Leunissen-Bijvelt, J., & De Gier, J. (1982) *Biochim. Biophys. Acta 692*, 126–138.
Van Lent, J. W. M., & Verduin, B. J. M. (1985) *Neth. J. Plant Pathol. 91*, 205–213.
Verduin, B. J. M. (1974) *FEBS Lett. 45*, 50–54.
Verduin, B. J. M. (1978) *J. Gen. Virol. 39*, 131–147.
Vriend, G., Hemminga, M. A., Verduin, B. J. M., De Wit, J. L., & Schaafsma, T. J. (1981) *FEBS Lett. 134*, 167–171.
Vriend, G., Hemminga, M. A., & Verduin, B. J. M. (1986) *J. Mol. Biol. 191*, 453–460.
Wang, C.-Y., & Huang, L. (1984) *Biochemistry 23*, 4409–4416.
Watts, J. W., & King, J. M. (1984) *J. Gen. Virol. 65*, 1709–1712.
Watts, W. J., Dawson, J. R. O., & King, J. M. (1981) *CIBA Found. Symp. 80*, 56–71.
Wilschut, J., & Hoekstra, D. (1986) *Chem. Phys. Lipids 40*, 145–166.
Wilson, T. M. A. (1984) *Virology 137*, 255–265.
Wilson, T. M. A. (1985) *J. Gen. Virol. 66*, 1201–1207.

Estimation by Radiation Inactivation of the Size of Functional Units Governing Sendai and Influenza Virus Fusion†

Keiko Bundo-Morita, Suzanne Gibson, and John Lenard*
Department of Physiology and Biophysics, UMDNJ-Robert Wood Johnson Medical School,‡ Piscataway, New Jersey 08854-5635

Received January 2, 1987; Revised Manuscript Received April 29, 1987

ABSTRACT: The target sizes associated with fusion and hemolysis carried out by Sendai virus envelope glycoproteins were determined by radiation inactivation analysis. The target size for influenza virus mediated fusion with erythrocyte ghosts at pH 5.0 was also determined for comparison; a value of 57 ± 15 kDa was found, indistinguishable from that reported previously for influenza-mediated fusion of cardiolipin liposomes [Gibson, S., Jung, C. Y., Takahashi, M., & Lenard, J. (1986) *Biochemistry 25*, 6264–6268]. Sendai-mediated fusion with erythrocyte ghosts at pH 7.0 was likewise inactivated exponentially with increasing radiation dose, yielding a target size of 60 ± 6 kDa, a value consistent with the molecular weight of a single F-protein molecule. The inactivation curve for Sendai-mediated fusion with cardiolipin liposomes at pH 7.0, however, was more complex. Assuming a "multiple target–single hit" model, the target consisted of 2–3 units of ca. 60 kDa each. A similar target was seen if the liposomes contained 10% gangliosides or if the reaction was measured at pH 5.0, suggesting that fusion occurred by the same mechanism at high and low pH. A target size of 261 ± 48 kDa was found for Sendai-induced hemolysis, in contrast with influenza, which had a more complex target size for this activity (Gibson et al., 1986). Sendai virus fusion thus occurs by different mechanisms depending upon the nature of the target membrane, since it is mediated by different functional units. Hemolysis is mediated by a functional unit different from that associated with erythrocyte ghost fusion or with cardiolipin liposome fusion.

Radiation analysis has been used previously to determine the inactivation target size for several functions of the influenza virus membrane (Gibson et al., 1986). Fusion of influenza with cardiolipin (CL)[1] liposomes was exponentially inactivated as a function of increasing radiation dose, corresponding to a radiation target size of 53–55 kDa, in reasonable agreement with the molecular weight of a single molecule of the influenza fusion protein HA. On the other hand, the targets governing

† This research was supported in part by Grant AI-13002 from the National Institutes of Health.
‡ Formerly Rutgers Medical School.

[1] Abbreviations: CL, cardiolipin; R_{18}, octadecylrhodamine B chloride; RET, resonance energy transfer; N-NBD-PE, *N*-(7-nitro-2,1,3-benzoxadiazol-4-yl)dipalmitoyl-L-α-phosphatidylethanolamine; N-Rh-PE, *N*-(lissamine rhodamine B sulfonyl)dioleoylphosphatidylethanolamine; Hepes, *N*-(2-hydroxyethyl)piperazine-*N*′-2-ethanesulfonic acid; EDTA, ethylenediaminetetraacetic acid.

0006-2960/87/0426-6223$01.50/0